

mostly eliminates this effect.

DENSITY MATRIX SIMULATIONS OF THE GAIN MEDIUM

To verify that our interpretation of the gain and phase dynamics are reasonable, we perform here simplified density-matrix simulations [5–7] of the electron transport and linear susceptibility of the gain medium. We incorporate eight states in our model and assume that scattering is dominated by LO phonon scattering, with an electron temperature that is 80 K higher than the lattice temperature [6]. In addition, we assume that different states decohere with a phenomenological pure dephasing rate of $T_2^* = 1$ ps, which takes into account the various un-modeled scattering mechanisms and is responsible for the majority of the linewidth broadening. A disadvantage to this approach is that all of the spectroscopically-accessible transitions have linewidths which are roughly the same, since at low temperatures the broadening due to LO phonon scattering is relatively small. In addition, because we do not incorporate the feedback of the cavity, we are only calculating the small-signal susceptibility and cannot observe gain clamping. The advantage to this approach is that it has only a single fitting parameter (i.e., the pure dephasing rate).

Figure S2 shows the simulated data corresponding to Fig. 2. Because the design bias of the real laser differs from the design bias of the simulated laser (due to growth imperfections and the QCL's contact), the simulated voltages are plotted over a range of 6.1 V to 8.3 V. The resulting gain and phase spectra agree reasonably well with the measured data, although some differences in the transition frequencies and lineshapes are apparent. In particular, the calculated transition frequencies are all moderately lower than the actual transition frequencies—a consequence of growth imperfections—and the calculated full-width half maximums of B and C are approximately the same—a consequence of their common pure dephasing rate.

One may also notice that the measured gain spectra shown in Fig. 2 exhibit less of a frequency shift with bias than would be predicted by the computed band structure. This is most clearly evident in transition A, which shows a strong shift in simulation but essentially none in measurement. In fact, the fitting procedure used to calculate the individual intersubband contributions in Fig. 3(c) implicitly assumed that the transition energies were static over the dynamic range of interest. This can be understood as a consequence of the electrical properties of resonant-phonon QCLs. Because several states of the laser need to be in alignment to conduct current through the structure, near design bias space charge will tend to hold the voltage across the structure relatively constant, and only the intersubband populations will change. Indeed, nanoscale imaging of the potential distribution of THz QCLs [8] has shown that because of domain formation, the actual electric field established in some portion of the device can remain constant, even as the applied field is changed. Of course, this assumption ceases to be valid over a larger dynamic range.

REFERENCES

1. D. Burghoff, T. Y. Kao, D. Ban, A. W. M. Lee, Q. Hu, and J. Reno, "A terahertz pulse emitter monolithically integrated with a quantum cascade laser," *Applied Physics Letters* **98**, 061112 (2011).
2. M. Martl, J. Darmo, C. Deutsch, M. Brandstetter, A. M. Andrews, P. Klang, G. Strasser, and K. Unterrainer, "Gain

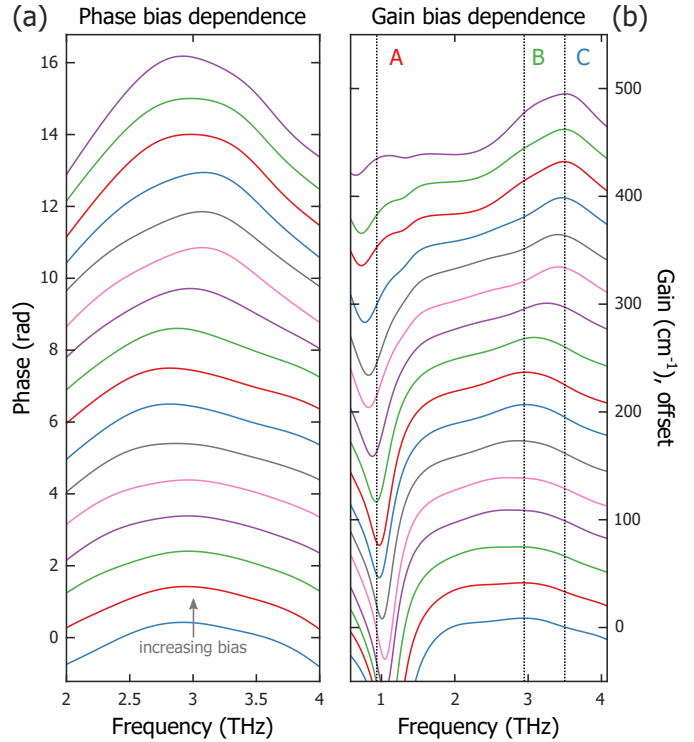


Fig. S2. (a) Round-trip phase of a 400 μm long laser at 48 K, calculated using a simplified density matrix formalism. The static contribution of dispersion has been added to the intersubband contribution. (a) Intersubband gain, with the three primary transitions highlighted.

- and losses in THz quantum cascade laser with metal-metal waveguide," *Optics Express* **19**, 733–738 (2011).
3. D. Burghoff, C. W. I. Chan, Q. Hu, and J. L. Reno, "Gain measurements of scattering-assisted terahertz quantum cascade lasers," *Applied Physics Letters* **100**, 261111 (2012).
4. D. P. Burghoff, "Broadband terahertz photonics," Ph.D. thesis pp. 69–70 (2014).
5. S. Kumar and Q. Hu, "Coherence of resonant-tunneling transport in terahertz quantum-cascade lasers," *Physical Review B* **80**, 245316 (2009).
6. G. Scalari, M. I. Amanti, C. Walther, R. Terazzi, M. Beck, and J. Faist, "Broadband THz lasing from a photon-phonon quantum cascade structure," *Optics Express* **18**, 8043–8052 (2010).
7. E. Dupont, S. Fatholouloumi, and H. C. Liu, "Simplified density-matrix model applied to three-well terahertz quantum cascade lasers," *Physical Review B* **81**, 205311 (2010).
8. R. S. Dhar, S. G. Razavipour, E. Dupont, C. Xu, S. Laframboise, Z. Wasilewski, Q. Hu, and D. Ban, "Direct nanoscale imaging of evolving electric field domains in quantum structures." *Scientific Reports* **4**, 7183 (2014).